Electronic Supplementary Information

Interface regulation of the Zn anode by using a low concentration electrolyte additive for aqueous Zn batteries

Kuo Wang[a,d], Qianrui Li[a,d], Guoli Zhang[a], Shuo Li[a], Tong Qiu[a], Xiao-Xia Liu[a,b,c] and Xiaoqi Sun[a,b,*]

[a.] Department of Chemistry, Northeastern University, Shenyang 110819, China.

[b.] National Frontiers Science Center for Industrial Intelligence and Systems Optimization, Northeastern University, 3-11 Wenhua Road, Shenyang, 110819, China.

[c.] Key Laboratory of Data Analytics and Optimization for Smart Industry (Northeastern University), Ministry of Education, China.

[d.] These authors contributed equally to this work.

*Corresponding author. E-mail: sunxiaoqi@mail.neu.edu.cn

1 Experimental procedures

1.1 Preparation of $V_6O_{13}·H_2O$

$V_6O_{13}·H_2O$ was synthesized according to a reported method.[1] In a typical synthesis, 2.73 g V_2O_5 and 4.52 g $H_2C_2O_4$ were added into 40 mL deionized water. The mixture was stirred at 90 °C for 1 h and transferred into a Teflon-lined autoclave. Subsequently, 10 mL H_2O_2 and 30 mL ethanol were added. The autoclave was heated at 180 °C for 3 h. After cooling down to room temperature, the product was filtered, washed with deionized water and ethanol, and dried at 60 °C under vacuum overnight.

1.2 Characterizations

^{67}Zn nuclear magnetic resonance (NMR) was carried out on a Bruker 600 MHz NMR spectrometer (Germany). Contact angles were measured on JY-82. X-ray diffraction (XRD) was measured on a PANalytical Empyrean diffractometer with Cu Kα radiation. The morphology was obtained by a SU8010 scanning electron microscope (HITACHI, Japan) and JEM-2100Plus transmission electron microscope (Japan). X-ray photoelectron spectroscopy (XPS) was performed on K-Alpha (Thermo Scientific, America). The data was analyzed using CasaXPS software and calibrated by referencing the C 1s peak to 284.8 eV.

1.3 Electrochemical measurements

The electrochemical performance of Zn//Zn, Zn//Cu and Zn//$V_6O_{13}·H_2O$ cells were tested in 2032 coin-type cells. Zn foil with 99.9% purity was obtained from Shanghai Sinopharm Chemical Reagent Co., Ltd. The $V_6O_{13}·H_2O$ cathode was prepared mixing the active material, Super P and PVDF at a mass ratio of 6:3:1 in N-Methyl pyrrolidone (NMP) and drop casted on graphite foil substrate. Cyclic voltammetry (CV) for electrochemical double layer capacitance (EDLC) analysis was performed in Zn//Zn Swagelok® cells. The EDLC values were obtained by the linear fits of *i*-*v* plots according to the equation of $C_{dl} = i/v$. Chronoamperometry (CA) measurements were performed in three-electrode cells with Zn foil as the working, counter and reference electrodes. All electrochemical measurements were performed on Bio-logic VMP3 or LANHE CT2001A battery test systems.

1.4 Computational methods

For molecular dynamic (MD) simulations, the model was constructed with 556 H_2O, 20 $ZnSO_4$ and 1 ASA, which agreed with the composition in the 0.1-ASA electrolyte. The COMPASSII forcefields were selected for assigning the charges for Zn^{2+}, SO_4^{2-} and

ASA. The geometry optimization was carried out in the Forcite module, in which the lattice geometry was optimized based on the convergence of total energy (0.001 kcal mol^{-1}). MD simulations were then conducted by NVT and NPT ensembles at 298 K. All simulations were carried out with the standard periodic boundary condition and the simulation time was long enough to ensure the equilibrium states of electrolyte systems.

The binding energy calculations were conducted in the Gaussian 16 program. The structure optimizations were performed at the B3LYP/6–31G(d,p) level.

The binding energies between Zn^{2+} and different solvent molecules were calculated by the following equation:

$$E_b = E_{molecule+Zn(2+)} - E_{molecule} - E_{Zn(2+)}$$

E_b was binding energy between Zn^{2+} and solvent molecule. $E_{molecule+Zn(2+)}$, $E_{molecule}$ and $E_{Zn(2+)}$ were the energies of Zn^{2+}-solvent complex, solvent molecule and Zn^{2+}, respectively.

The adsorption energies of solvent molecules on Zn, charge density difference, LUMO energies and relative energies of solvation structure were calculated by the DMol3 program package in Materials Studio. The exchange and correlation terms were determined using the Generalized Gradient Approximation (GGA) in the form proposed by Perdew, Burke, and Ernzerhof (PBE). The energy convergence criterion was set to 10^{-6} Hartree. All calculations including geometry optimization, single-point energy and electronic density were carried out under a periodic boundary condition. In the Z direction, there was about 15 Å vacuum for erasing the effect of periodic condition for slab model. A 5*5 supercell with four layers of Zn (002) face were used to represent the adsorbed surface.

The adsorption energies of different solvent molecules on Zn slab were calculated by the following equation:

$$E_{adsorb} = E_{molecule+Zn} - E_{molecule} - E_{Zn}$$

E_{adsorb} was the adsorption energy. $E_{molecule+Zn}$, $E_{molecule}$ and E_{Zn} were the energies of the system, solvent molecule and Zn, respectively.

2 Supplementary Figures and Table

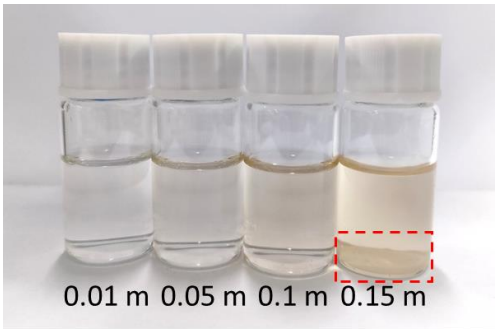

Figure S1. Digital photos of the 2 m $ZnSO_4$ electrolytes with different concentrations of ASA additive.

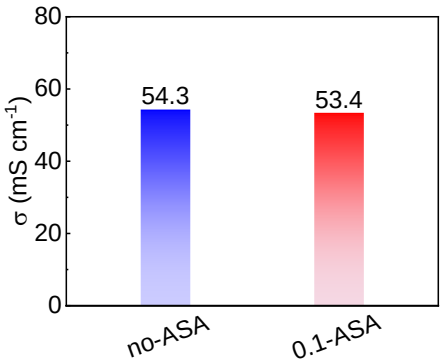

Figure S2. Ionic conductivities of 2 m $ZnSO_4$ solution and with 0.1 m ASA additive.

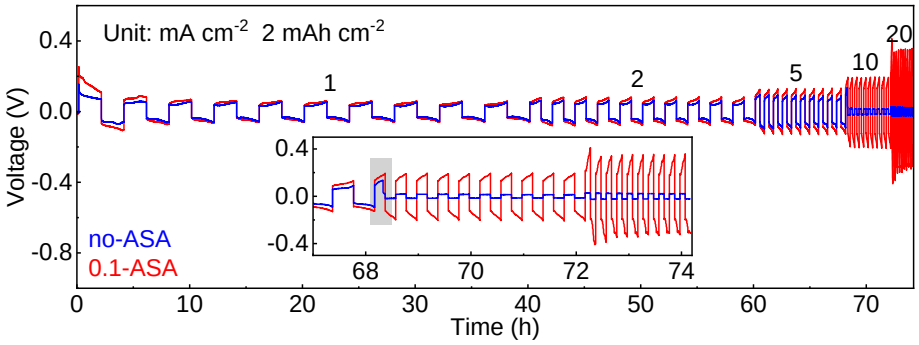

Figure S3. The rate performance of Zn//Zn symmetric cells in the two electrolytes.

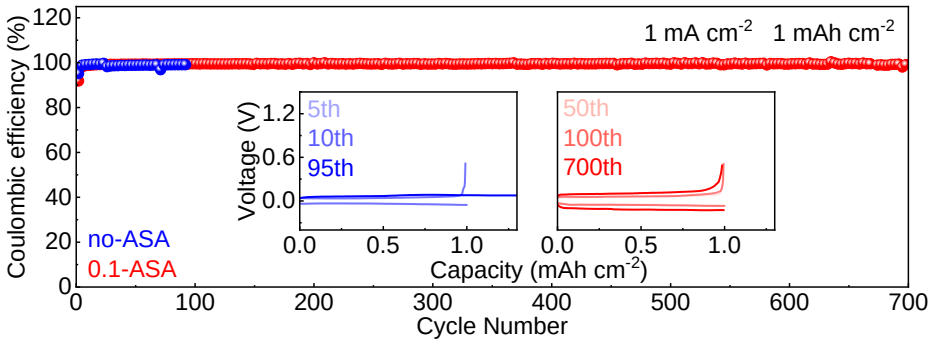

Figure S4. Coulombic efficiencies of Zn plating-stripping in Zn//Cu cells with the two electrolytes at 1 mA cm^{-2} and 1 mAh cm^{-2}.

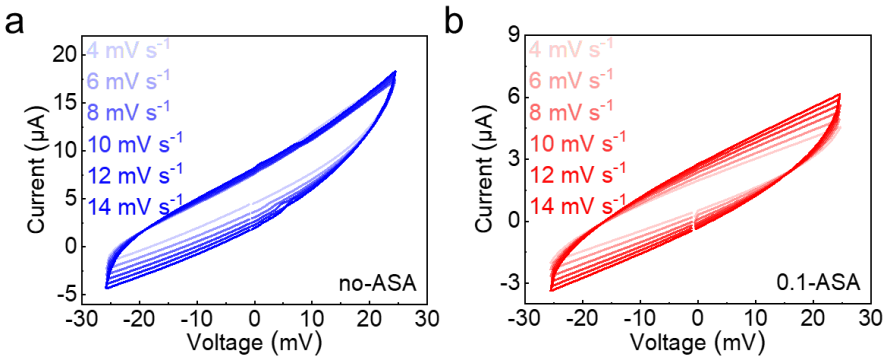

Figure S5. CV curves of Zn//Zn symmetric cells in the non-Faradic range in a) 2 m $ZnSO_4$ and b) 0.1 m ASA electrolytes.

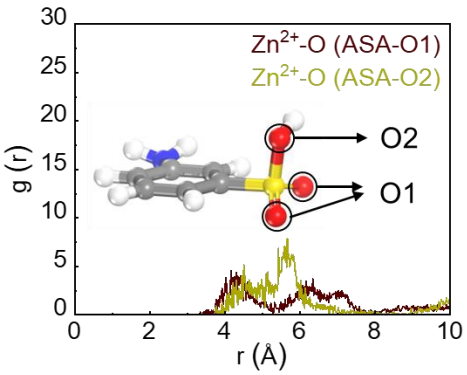

Figure S6. RDFs for the interactions of Zn^{2+} and different O sites on ASA in the 0.1-ASA electrolyte.

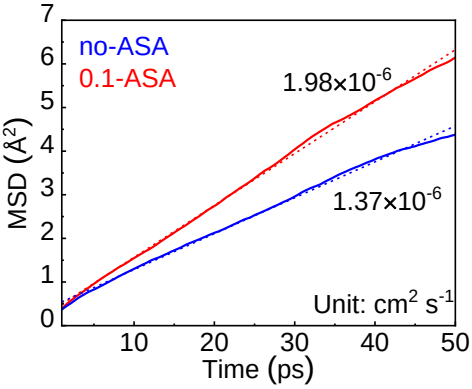

Figure S7. MSD plots of the two electrolytes.

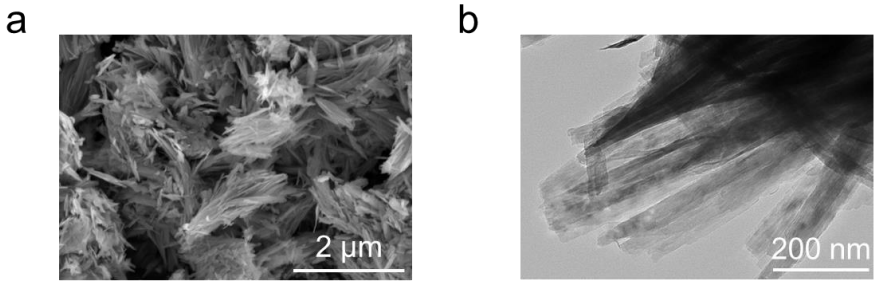

Figure S8. a) SEM and b) TEM images of $V_6O_{13}·H_2O$.

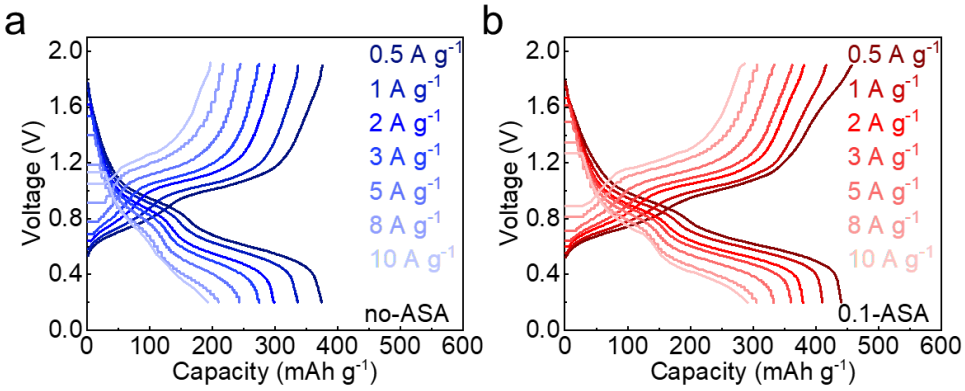

Figure S9. Charge/discharge curves of $V_6O_{13}·H_2O$ at different current densities with the electrolytes of (a) 2 m $ZnSO_4$ and (b) with 0.1 m ASA additive.

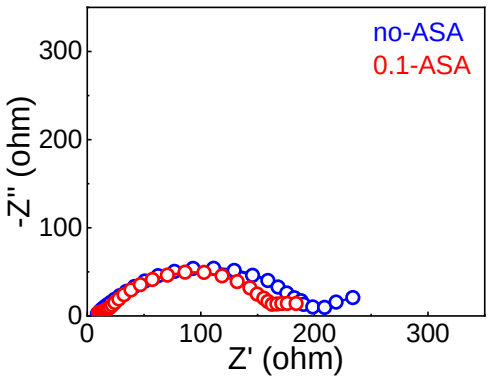

Figure S10. Nyquist plots of the $V_6O_{13}·H_2O$ cathode in different electrolytes.

Table S1. Electrochemical performance comparison of symmetric Zn cells using electrolytes containing different additives.

Electrolyte Additive	Additive amount (% relative to H_2O)	Current density (mA cm^{-2})	Areal capacity (mAh cm^{-2})	Cycling life (h)	Refs.
Glycerol	50%	2	2	700	[2]
EG	44.5%	2	1	150	[3]
Glycine	29.1%	5	1	700	[4]
DMSO	22.6%	0.5	0.5	1000	[5]
TMA	17.9%	5	2.5	500	[6]
TG	10.0%	2	0.67	1000	[7]
AN	8.7%	1	2	600	[8]
NMP	5.1%	1	1	550	[9]
LiCl	9.3%	1	1	125	[10]
ASA	1.7%	2	2	1100	This work
		5	5	600	
		10	2	400	

3 References

1. J. Lai, H. Zhu, X. Zhu, H. Koritala and Y. Wang, Interlayer-Expanded $V_6O_{13}·nH_2O$ Architecture Constructed for an Advanced Rechargeable Aqueous Zinc-Ion Battery, ACS Appl. Energy Mater. 2019, 2, 1988-1996.
2. Y. Zhang, M. Zhu, K. Wu, F. Yu, G. Wang, G. Xu, M. Wu, H. K. Liu, S. X. Dou, C. Wu, An in-depth insight of a highly reversible and dendrite-free Zn metal anode in an hybrid electrolyte, J. Mater. Chem. A, 2021, 9, 4253–4261.
3. N. Chang, T. Li, R. Li, S. Wang, Y. Yin, H. Zhang, X. Li, An aqueous hybrid electrolyte for low-temperature zinc-based energy storage devices, Energy Environ. Sci., 2020, 13, 3527–3535.
4. Yang, F., Yuwono, J. A., Hao, J., Long, J., Yuan, L., Wang, Y., Liu, S., Fan, Y., Zhao, S., Davey, K., Guo, Z., Understanding H_2 Evolution Electrochemistry to Minimize Solvated Water Impact on Zinc-Anode Performance, Adv. Mater., 2022, 34, 2206754.
5. L. Cao, D. Li, E. Hu, J. Xu, T. Deng, L. Ma, Y. Wang, X. Q. Yang, C. Wang, Solvation Structure Design for Aqueous Zn Metal Batteries, J. Am. Chem. Soc., 2020, 142, 21404–21409.
6. Yao, R., Qian, L., Sui, Y., Zhao, G., Guo, R., Hu, S., Liu, P., Zhu, H., Wang, F., Zhi, C., Yang, C., A Versatile Cation Additive Enabled Highly Reversible Zinc Metal Anode, Adv. Energy Mater., 2022, 12, 2102780.
7. Liu, Z., Wang, R., Ma, Q., Wan, J., Zhang, S., Zhang, L., Li, H., Luo, Q., Wu, J., Zhou, T., Mao, J., Zhang, L., Zhang, C., Guo, Z., A Dual-Functional Organic Electrolyte Additive with Regulating Suitable Overpotential for Building Highly Reversible Aqueous Zinc Ion Batteries, Adv. Funct. Mater., 2023, 2214538.
8. Z. Hou, H. Tan, Y. Gao, M. Li, Z. Lu, B. Zhang, Tailoring desolvation kinetics enables stable zinc metal anodes, J. Mater. Chem. A, 2020, 8, 19367–19374.
9. T. C. Li, Y. Lim, X. L. Li, S. Luo, C. Lin, D. Fang, S. Xia, Y. Wang, H. Y. Yang, A Universal Additive Strategy to Reshape Electrolyte Solvation Structure toward Reversible Zn Storage, Adv. Energy Mater. 2022, 12, 2103231.
10. X.-X. Guo, Z.-Y. Zhang, J.-W. Li, N.-J. Luo, G.-L. Chai, Thomas S. Miller, F.-L. Lai, Paul Shearing, Dan J. L. Brett, D.-L Han, Z. Weng, G.-J. He, and Ivan P. Parkin, Alleviation of Dendrite Formation on Zinc Anodes via Electrolyte Additives, ACS Energy Letters, 2021 6 (2), 395-403.